Three-dimensional spinning solitons in dispersive media with the cubic-quintic nonlinearity

Anton Desyatnikov,[1,*] Andrey Maimistov,[1,†] and Boris Malomed[2,‡]
[1]*Department of Solid State Physics, Moscow Engineering Physics Institute, Moscow 115409, Russia*
[2]*Department of Interdisciplinary Studies, Faculty of Engineering, Tel Aviv University, Tel Aviv 69978, Israel*
(Received 9 July 1999)

We study spatiotemporal three-dimensional bright solitons in optical media whose non-linear response includes third- and fifth-order terms. By means of numerical simulations, lower and upper stability and existence borders for the solitons without the internal ''spin'' are identified. Using the variational method based on two different trial functions and collating the results, we obtain approximate solutions for *spinning* (vortex) solitons. The presence of the lower stability border for both the zero-spin and spinning solitons is a drastic difference of the three-dimensional solitons from those in one and two dimensions. The results show that the corresponding stability and existence borders are chiefly determined by the spatial dimension, quite weakly depending on the soliton's ''spin.'' However, the energy of the spinning soliton is much larger than that of the zero-spin one.

PACS number(s): 42.65.Tg

I. INTRODUCTION

Optical spatiotemporal solitons, or the so-called light bullets (LB's) [1–7], have been attracting a growing interest in the last decade, as they are expected to be a new fundamental physical object, and also have a potential to implement ultrafast all-optical switching in a bulk medium [8–12]. Various effects generated by interactions between the spatiotemporal solitons, such as scattering, fusion, repulsion, and spiraling, have also been theoretically studied [8,9,13–16].

It is well known that in the Kerr medium with a purely cubic nonlinear response, LB's formally exist, but, in both the two- and three-dimensional (2D and 3D) cases, they are unstable against the spatiotemporal collapse induced by a combined effect of the nonlinearity and anomalous dispersion [3]. To prevent the collapse, it is necessary to change the nonlinearity. One possibility is to consider media with a quadratic (second-harmonic generating) nonlinearity [12]. The theoretical work in this direction, begun long ago [1] and continued recently [12], has finally led to the experimental observation of a LB. In fact, the observed object was a quasi-2D bullet in a 3D sample of the $LiIO_3$ optical crystal. The size of the sample was $\sim$1 cm. Work aimed at the observation of a fully localized 3D bullet in the same medium is now in progress [17].

Alternatively, the collapse can be checked by a saturation of the Kerr response [18–20]. The dependence of the nonlinear correction to the refractive index on the light intensity I is then

$$n_{\rm nl}=n_K I(1+I/I_s)^{-1}, \tag{1}$$

where n_K is the Kerr coefficient, and I_s is the saturation intensity. For this model, the existence and stability of 2D axisymmetric ''bullets'' (spatiotemporal solitons) has been known for a long time [21]; 3D spherically symmetric solitons and their stability in the same model were studied in detail by Edmundson [22]. Note, however, that higher-order soliton modes, consisting of a dark spot that is surrounded by bright rings, were numerically found to be unstable in the 2D saturable model [23].

For weak fields, $I/I_s \ll 1$, Eq. (1) yields the usual self-focusing Kerr response, $n_{\rm nl}\approx n_K I$. With the increase of the intensity, it is necessary to take into consideration the next-order *self-defocusing* term in the expansion of the full refractive index:

$$n=n_0+n_2 I-n_4 I^2, \tag{2}$$

where n_0 is its linear part, $n_2\equiv n_K$, and $n_4\equiv 2n_K/I_s$.

Although the *cubic-quintic* (with respect to the field amplitude, see below) dependence $n(I)$ corresponding to Eq. (2) was obtained from the expansion of the saturable dependence (1) for small values of the intensity, it makes sense to consider the cubic-quintic model (2) as an independent one, valid beyond the framework of applicability of the expansion to Eq. (1) [24,13]. This is stimulated, in particular, by the fact that the dependence $n(I)$ in a form well approximated by Eq. (2) has been found experimentally in some organic materials [25]. From the theoretical viewpoint, there is a drastic difference between the saturable and cubic-quintic models. As was demonstrated long ago by Kolokolov [26], the (nonspinning) spatiotemporal solitons in the former model are stable, because the model satisfies the self-focusing condition $dn/dI>0$ at all values of I. Obviously, this is not the case for the cubic-quintic model; hence the solitons' stability must be studied separately in this model. It is noteworthy that the quintic term, while preventing the collapse, causes only a small change in the effective potential of the interaction between far-separated spatiotemporal solitons [14,15].

An equation governing the evolution of the envelope E of the electromagnetic field ($I=|E|^2$) in a nonlinear isotropic

*Electronic address: anton@edu.dp.ua
†Electronic address: maimistov@pico.mephi.ru
‡Electronic address: malomed@eng.tau.ac.il

dispersive medium, where the refractive index is taken in the form (2), is the cubic-quintic nonlinear Schrödinger (CQNLS) equation:

$$2i\kappa E_z+\nabla_\perp^2 E+\kappa D E_{TT}+2\kappa^2(n_2/n_0)|E|^2E - 2\kappa^2(n_4/n_0)|E|^4E=0, \quad (3)$$

where κ is the propagation constant (wave number), $D=-d^2\kappa/d\omega^2>0$ is the coefficient of the temporal dispersion, which is assumed *anomalous* (there is no chance to have solitons if the dispersion is normal, with $D<0$), $T\equiv t-z/v_g$ (v_g being the group velocity of the carrier wave) is the ''reduced time,'' and the Laplacian $\nabla_\perp^2$ (representing the spatial diffraction) acts on the transverse coordinates.

Defining rescaled variables $u=E\sqrt{n_4/n_2}$, $\tau=Tn_2\sqrt{2\kappa/Dn_0n_4}$, $\zeta=z\kappa n_2^2/n_0n_4$, and $(\xi,\eta)=(x,y)\kappa n_2\sqrt{2/n_0n_4}$, one transforms Eq. (3) into a normalized form:

$$iu_\zeta+\nabla^2u+|u|^2u-|u|^4u=0, \quad (4)$$

where $\nabla^2=\partial^2/\partial\xi^2+\partial^2/\partial\eta^2+\partial^2/\partial\tau^2$ is the *spatiotemporal* Laplacian. Note that, like the usual cubic NLS equation, the normalized CQNLS equation (4) contains no dimensionless parameters. Nevertheless, soliton solutions to Eq. (4) have an important difference from those found for the Kerr media; namely, the NLS equation admits an obvious rescaling of solutions without changing the form of the equation. This makes it possible for a single soliton to represent all the soliton solutions [3]. The situation is different for the CQNLS equation, in which rescaling the variables without a change of the equation's form is impossible. Therefore, it is necessary to search numerically for a whole family of solutions, by varying values of a properly defined control parameter. This was done for 2D bright vortex solitons, i.e., localized solutions with an internal vorticity (''spin'') 1, in Ref. [13]. Later, the analysis was extended to 2D solitons with zero spin [27].

The most remarkable property of the 2D vortex solitons in the CQNLS model, discovered by means of numerical simulations in Ref. [13], is their stability (note, however, the instability of a *helical* vortex soliton in the same model, with an amplitude periodically modulated along the propagation distance, which was reported in Ref. [28]). In sharp contrast with this, 2D vortex solitons in the model with the quadratic nonlinearity, although they exist as stationary solutions, are subject to a strong azimuthal instability, which was predicted numerically [29,30], and then observed experimentally [31]. A similar strong azimuthal instability of the 2D spinning soliton has been found in numerical simulations of the model with the saturable nonlinearity (1) [29]. The latter fact stresses a drastic difference between the saturable and cubic-quintic models.

The objective of this work is to find 3D soliton solutions of Eq. (4), i.e., the light bullets in the bulk cubic-quintic medium. In Sec. II, we numerically search for radially symmetric solitons without the spin. We find *two* branches in the dependence of the soliton's energy on its propagation constant (i.e., two different branches of the solutions), only one of them being stable. This dependence qualitatively (but not quantitatively) resembles the U-shaped curve known for the saturable model [22]. We determine a stability threshold for the soliton solutions, along with their existence boundary. In Sec. III, which is the core of this work, *spinning* 3D light bullets are studied by means of the variational approximation (VA). We find the corresponding solutions, using two essentially different versions of VA, and discuss their common properties and distinctions (with the conclusion that both predict crucially important properties in a nearly identical form). Similar to the zero-spin 3D solitons, and unlike the 2D vortex ones [13], the solution for the spinning 3D solitons has stable and unstable branches. The stability threshold for the solutions is found. In Sec. IV, we compare the properties of the 3D light bullets with and without spin. We conclude that, while the minimum (threshold) energy of the spinning soliton is more than four times as large as that of the zero-spin one, the stability threshold, defined in terms of the soliton's propagation constant, very weakly depends on the spin.

To conclude the introduction, it is relevant to briefly discuss how, in principle, the bullets may be generated in an experiment. For the zero-spin case, an incident laser pulse may self-trap into the bullet in the bulk medium, as was the case in the recent experiment [7]. To generate a spinning bullet, one may use a pulse that has passed through a specially shaped phase mask, which can lend the pulse the necessary vorticity, as was done in the work [31].

II. ZERO-SPIN SOLITONS

Following Ref. [3], we introduce the spatiotemporal radius

$$r=\sqrt{\xi^2+\eta^2+\tau^2} \quad (5)$$

and search for solutions to Eq. (4) in the form $u(\xi,\eta,\tau,\zeta)=\exp(ik\zeta)V(r)$. An equation for $V(r)$ can then be easily obtained:

$$V''+(2/r)V'-kV+V^3-V^5=0, \quad (6)$$

with the boundary conditions defined by means of asymptotic expressions,

$$V(r)\approx a(k)(1+\gamma r^2), \quad \gamma=(a^4-a^2+k)/6, \quad r\to 0, \quad (7)$$

$$V(r)\approx A(k)r^{-1}\exp(-\sqrt{k}r), \quad r\to\infty. \quad (8)$$

Figure 1 displays a set of solutions to Eq. (6), obtained, for different values of k, by means of the shooting method. It is noteworthy that the effective size of the soliton increases with the parameter k, i.e., contrary to what is suggested by the asymptotic expression (8), $k^{-1/2}$ is *not* an estimate for the soliton's size. With the increase of the size, the distribution of the field at the soliton's center becomes flatter. This corresponds to a decrease of the curvature parameter γ defined in Eq. (7). In the limit of $\gamma=0$, the soliton's amplitude a at $r=0$ assumes either of the two limiting values, which are, in fact, amplitudes of two plane-wave solutions to Eq. (4) with the same propagation constant k,

$$a_{1,2}(k)\equiv\sqrt{\tfrac{1}{2}(1\pm\sqrt{1-4k})}. \quad (9)$$

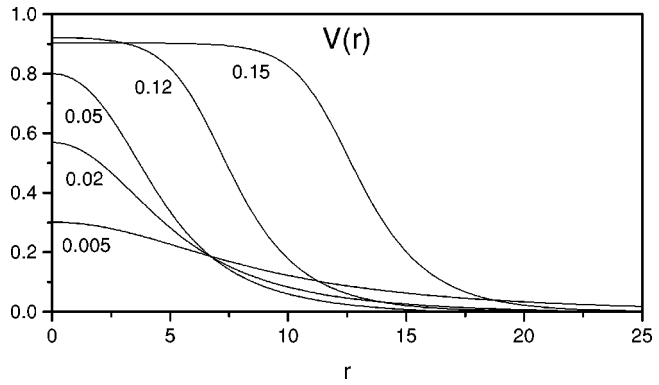

FIG. 1. The solutions for 3D solitons with zero spin. The values of the propagation constant k are indicated near the curves.

The dependence $a(k)$ found numerically for zero-spin solitons, together with that for plane waves, as given by Eq. (9), is shown in Fig. 2. It is seen from this figure that, with the increase of k, the amplitude $a(k)$ approaches $a_1(k)$, attaining this value at $k=k_{\max}^{(3D)}\approx 0.15$. Thus, $k=k_{\max}^{(3D)}$ is an *existence boundary* of the zero-spin solitons, at which the size of the soliton diverges as it is going over into a plane wave. This limitation on k may be regarded as a saturation of the propagation constant.

In any dimension, there is a similar *upper* boundary for the values of k at which solitons exist. In the 1D case, one has, instead of Eq. (6), an equation $V''-kV+V^3-V^5=0$, with the well-known exact soliton solution

$$V^2(X)=4k[1+\sqrt{1-(16/3)k}\cosh(2\sqrt{k}X)]^{-1}, \quad (10)$$

where X is the transverse coordinate. Obviously, the solution (10) exists at $k<k_{\max}^{(1D)}=\frac{3}{16}$, at $k=k_{\max}^{(1D)}$ the soliton amplitude coinciding with the larger plane-wave amplitude a_1 from Eq. (9). In the 2D case, we have found, using the same shooting method, $k_{\max}^{(2D)}\approx 0.18$. It is noteworthy that $k_{\max}^{(3D)}<k_{\max}^{(2D)}<k_{\max}^{(1D)}$; hence we conclude that the upper boundary of the existence of the soliton solutions to Eq. (4) decreases as the space dimension increases.

The most important physical characteristic of the 3D optical soliton is its energy,

$$E(k)=4\pi\int_0^\infty V^2(r;k)r^2dr. \quad (11)$$

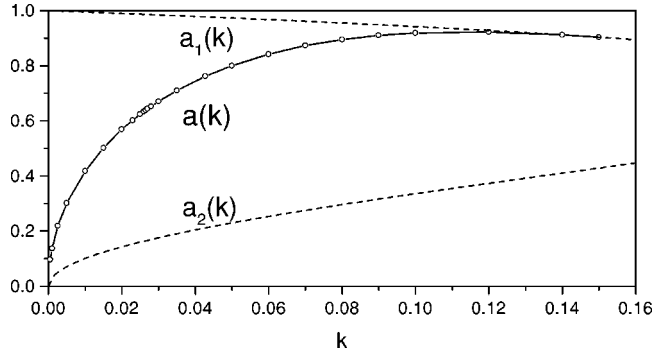

FIG. 2. The amplitude (at $r=0$) vs the propagation constant k for the 3D zero-spin soliton. The maximum of the amplitude is attained at $k\approx 0.12$.

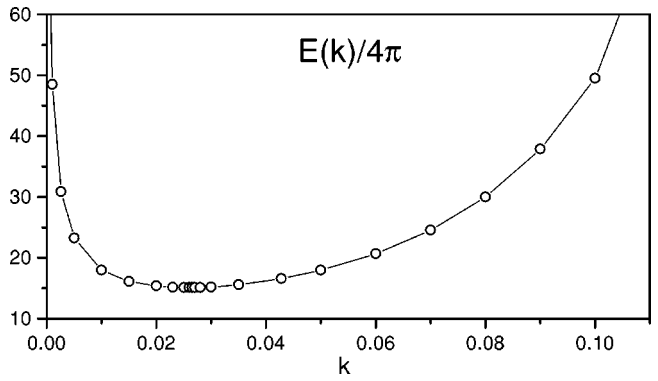

FIG. 3. The energy of the 3D zero-spin soliton vs its propagation constant.

Figure 3 displays the energy of the 3D LB vs k. A crucial difference of this dependence from those for the 1D and 2D solitons (in the same CQNLS model) is that the energy is *diverging* in the limit $k\to 0$. This is explained by the fact that, as seen in Fig. 1, although the soliton's amplitude vanishes as $k\to 0$, the soliton is quickly getting very broad. Because of the multiplier r^{D-1} in the expression for E [see Eq. (11)], the energy is very sensitive to the soliton's width. Our analysis of the same dependence in the 2D case shows that the energy (or the beam's power, if the 2D soliton is interpreted as a spatial cylindrical beam; see, e.g., Ref. [32]) attains a *finite* value $E_{\min}^{(2D)}\simeq 11.75$ at $k=0$, and in the 1D case the energy of the soliton given by Eq. (10) vanishes as $k\to 0$. An important consequence of the divergence of the 3D soliton's energy at $k\to 0$ is the presence of a *minimum energy* necessary for the existence of the 3D zero-spin solitons, whose numerical value is $E_{\min}/4\pi\approx 15$ (note a similar property of LB's in the model with the quadratic nonlinearity: they have nonzero $E_{\min}$ in both the cases $D=2$ and $D=3$ [12]).

Lastly, we notice that the U-shaped dependence $E(k)$ is tantamount to the existence of two soliton solutions, with different values of k, at each value of the energy $E>E_{\min}$. This is a distinctive feature of the 3D case, which is also known in the saturable model [21,22].

A necessary stability condition for solitons is given by the well-known Vakhitov-Kolokolov (VK) criterion [21,33]: the dependence $E(k)$ must have a positive slope, i.e., $dE/dk>0$. The fact that the energy of the 3D soliton diverges in both limits $k\to\infty$ and $k\to 0$ gives rise to a point $k_{\rm cr}\approx 0.026$, at which dE/dk changes its sign; see Fig. 3. Thus, the zero-spin 3D solitons are definitely unstable at $k<k_{\rm cr}$, and may be stable at $k>k_{\rm cr}$ (note that, in some cases, the Vakhitov-Kolokolov criterion turns out to be not only necessary, but also *sufficient* for the stability of the soliton [26,33]).

III. SOLITONS WITH SPIN ONE

A. *Ansätze* 1: Spherical variables

The spherical spatiotemporal coordinates, supplementing the radial variable r introduced in Eq. (5), can be applied to construct solutions to Eq. (4) in the form of 3D solitons with an integer spin $m\neq 0$. We search for such solutions as

$$u(\xi,\eta,\tau,\zeta)=\exp(ik\zeta+im\varphi)V(r,\theta), \tag{12}$$

where $\cos\theta\equiv\tau/r$, and φ is the usual angular coordinate in the transverse plane (ξ,η). Then, Eq. (4) is transformed into

$$\frac{1}{r^2}\frac{\partial}{\partial r}\left(r^2\frac{\partial V}{\partial r}\right)+\frac{1}{r^2\sin\theta}\frac{\partial}{\partial\theta}\left(\sin\theta\frac{\partial V}{\partial\theta}\right)-\frac{m^2V}{r^2\sin^2\theta}-kV+V^3-V^5=0. \tag{13}$$

This is the Euler-Lagrange equation $\delta S=0$, resulting from varying the action $S=\int_0^\infty dr\int_0^\pi L\,d\theta$ with the Lagrangian

$$L=\frac{1}{2}r^2\sin\theta\left\{\left(\frac{\partial V}{\partial r}\right)^2+\frac{1}{r^2}\left(\frac{\partial V}{\partial\theta}\right)^2+\frac{m^2V^2}{r^2\sin^2\theta}+kV^2-\frac{1}{2}V^4+\frac{1}{3}V^6\right\}. \tag{14}$$

Hereafter, we consider only the case $m=1$, as it does not seem plausible that a vortex soliton with $m>1$ can be dynamically stable. Note that it has been demonstrated that dark optical vortices (the ones whose field does not vanish at infinity) are definitely unstable if $m>1$ [34].

We aim to develop the variational approximation for a description of 3D spinning solitons (note that various forms of VA, using Gaussian and super-Gaussian *Ansätze*, or trial functions, were applied to the description of 1D solitons in the CQNLS model [35]). We here adopt the trial function

$$V(r,\theta)=U(r)\sin\theta, \tag{15}$$

which, as a matter of fact, represents nothing else but a spherical harmonic with the quantum numbers $l=1$ and $m=1$. Of course, it cannot be an exact solution to the nonlinear equation (13). One should also bear in mind that this is, in fact, not a spatial but a *spatiotemporal* spherical harmonic.

Inserting the *Ansätze* (15) into the Lagrangian (14) and integrating it over θ, but keeping an arbitrary dependence $U(r)$, one can readily derive the corresponding Euler-Lagrange equation,

$$\frac{d^2U}{dr^2}+\frac{2}{r}\frac{dU}{dr}-2\frac{U}{r^2}-kU+\frac{4}{5}U^3-\frac{24}{35}U^5=0. \tag{16}$$

Solutions to this equation pertaining to different values of k are displayed in Fig. 4. These solutions were found numerically by means of the shooting method adjusted to the obvious boundary conditions stating that $U(r)$ must vanish linearly at $r\to0$ and exponentially at $r\to\infty$. Similarly to the 2D case [13], it was found that the slope of the function $U(r)$ at $r=0$ increases with k up to a maximum value at $k=0.09$, and then decreases (in the 2D case, a maximum was attained at $k=0.145$).

The energy of the spinning soliton (12) is given by the expression

$$E=2\pi\int_0^\infty r^2dr\int_0^\pi\sin\theta\,d\theta\,V^2(r,\theta).$$

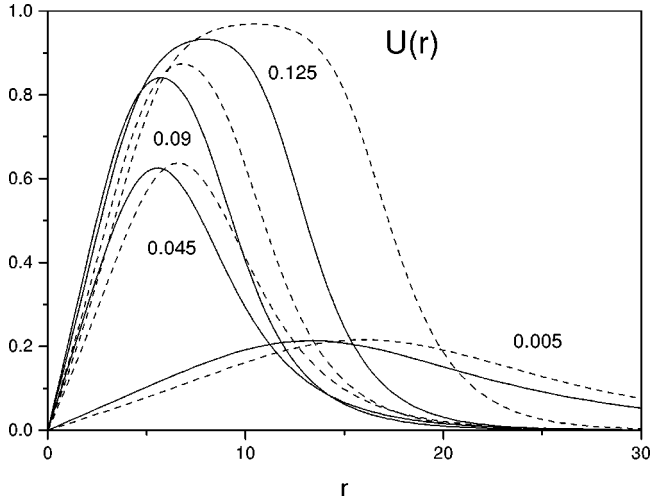

FIG. 4. Solutions for 3D spinning solitons with $m=1$. The solid and dashed curves show, respectively, the functions $U(r)$ and $U(\rho)$ [see Eqs. (15) and (21)] with the same values of k, which are written near the curves.

Substituting into this formula the *Ansätze* (15), one obtains [cf. Eq. (11)]

$$E(k)=(4\pi)^{\frac{2}{3}}\int_0^\infty U^2(r;k)r^2dr. \tag{17}$$

The energy given by the latter expression is displayed, as a function of the propagation constant k, in Fig. 5. The minimum of the function, $E_{\min}/4\pi\approx62.6$, is located at $k=k_{\rm cr}\approx0.033$. Consequently, the above-mentioned VK criterion [21] suggests that the spinning soliton with $m=1$ may be stable at $k>k_{\rm cr}$. Strictly speaking, the applicability of this criterion to vortex solitons, whose amplitude vanishes at the center, has not been proved, but recent results for the 2D vortex solitons in the present model [13] show that the numerically found stability indeed complies with the VK criterion. It is also noteworthy that the $k_{\rm cr}$ does not strongly depend on the spin: a similar value found in the previous section for $m=0$ was 0.026.

It was not possible to find soliton solutions to Eq. (16) at k exceeding some maximum value. Within the accuracy of the numerical calculations (and of the accuracy provided by the VA), this value proves to coincide with $k_{\rm max}^{(3D)}\approx0.15$,

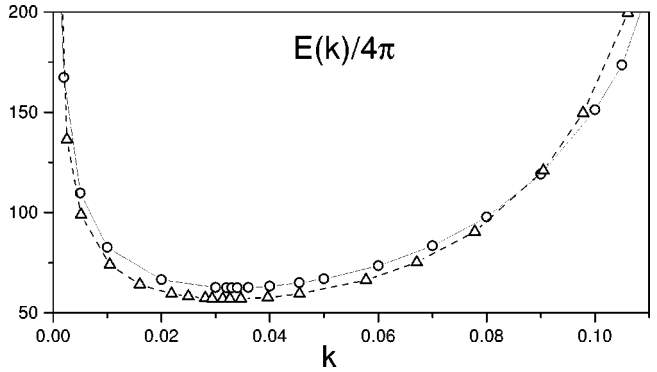

FIG. 5. The energy of the 3D spinning soliton. The circles and triangles indicate numerical values obtained, respectively, for the spherical and cylindrical *Ansätze* [see Eqs. (17) and (31)].

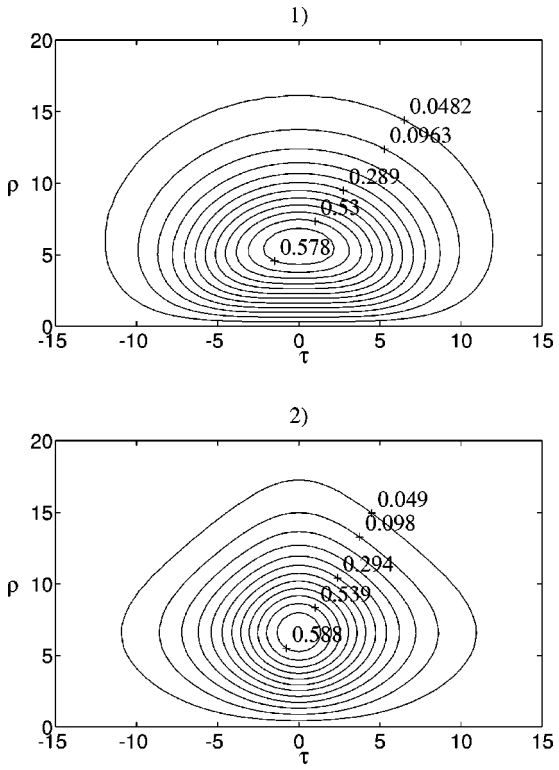

FIG. 6. Distribution of the 3D spinning soliton's field (shown by means of the level contours) in the plane (ρ,τ) at $k=0.045$: (1) the spherical *Ansätze*; (2) the cylindrical *Ansätze*.

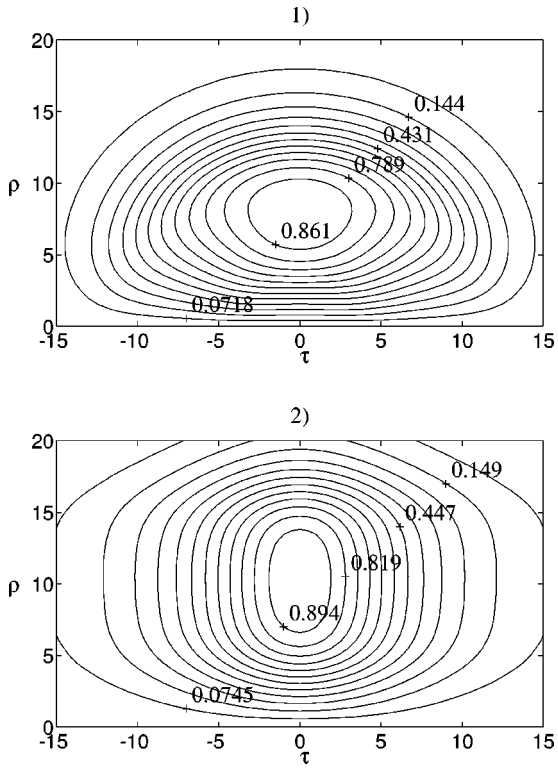

FIG. 7. The same as Fig. 6 at $k=0.125$.

which was the upper existence border for the zero-spin solitons found in the previous section. Thus, the upper existence bound (in terms of the propagation constant) for multidimensional solitons does not depend strongly on the value of the spin, but it depends upon the spatial dimension: we have checked that the upper bounds almost coincide too for 2D solitons with $m=0$ and $m=1$ (both are $k_{\max}^{(2D)}\approx 0.18$; see also Ref. [13] for the case $m=1$).

The ratio of the minimum energies of the $m=0$ and $m=1$ solitons in the 2D case (which are $E_{\min}^{(2D)}\simeq 50$ for the soliton with $m=1$ [13] and $E_{\min}^{(2D)}\simeq 11.75$ for the zero-spin soliton) is $50/11.75\simeq 4.26$. Comparing this to the same ratio in the 3D case, $62.6/15\simeq 4.17$, allows us to conclude that, in any dimension, formation of a spinning soliton requires energy which is, roughly, four times that necessary for the formation of a spinless soliton. Thus, experimental generation of the spinning soliton is expected to be harder than of the zero-spin one, but not impossible.

Lastly, the distribution of the spinning soliton's field in the plane $(\rho\equiv\sqrt{\xi^2+\eta^2},\tau)$ (i.e., a cross-section at $\varphi=\text{const}$) for two characteristic values of k is displayed in Figs. 6 and 7.

B. *Ansätze* 2: Cylindrical variables

We will now consider an alternative approximation for the description of essentially the same solution, i.e., the spinning 3D soliton. Here, we introduce the cylindrical spatiotemporal variables (ρ,φ,τ), where $\rho=r\sin\theta$ [in terms of the spatial variables, $\rho\equiv\sqrt{\xi^2+\eta^2}$, i.e., ρ is the usual radial coordinate in the transverse 2D plane (ξ,η)]. This time, a stationary solution is sought for in the form (we again confine ourselves to the case $m=1$)

$$u(\xi,\eta,\tau,\zeta)=\exp(ik\zeta+i\varphi)V(\rho,\tau), \tag{18}$$

cf. Eq. (12). The substitution of this into Eq. (4) yields

$$\frac{\partial^2 V}{\partial\rho^2}+\frac{1}{\rho}\frac{\partial V}{\partial\rho}+\frac{\partial^2 V}{\partial\tau^2}-\frac{V}{\rho^2}-kV+V^3-V^5=0. \tag{19}$$

We stress that both Eqs. (13) (with $m=1$) and (19) are exact and tantamount to each other. However, their approximate solutions generated by VA are *not* equivalent. Actually, comparison between them offers a convenient opportunity to estimate the accuracy and reliability of the VA.

The variational representation of Eq. (19) is $\delta S=0$, with $S=\int_0^\infty d\rho\int_{-\infty}^{\infty}L\,d\tau$, where

$$L=\frac{\rho}{2}\left\{\left(\frac{\partial V}{\partial\rho}\right)^2+\left(\frac{\partial V}{\partial\tau}\right)^2+\frac{V^2}{\rho^2}+kV^2-\frac{1}{2}V^4+\frac{1}{3}V^6\right\}. \tag{20}$$

To apply the VA to this problem, we follow the work [6] and adopt an *Ansätze* assuming the separation of the variables ρ and τ:

$$V(\rho,\tau)=U(\rho)\,\mathrm{sech}(\mu\tau), \tag{21}$$

where the inverse temporal width μ is a variational parameter. The Lagrangian (20), integrated over the variable τ, yields an *averaged Lagrangian*,

$$\langle L\rangle=\frac{\rho}{\mu}\left\{\left(\frac{dU}{d\rho}\right)^2+\frac{U^2}{\rho^2}+\beta U^2-\frac{1}{3}U^4+\frac{8}{45}U^6\right\}, \tag{22}$$

$$\beta\equiv k+\mu^2/3. \tag{23}$$

The standard variational procedure applied to the latter Lagrangian yields the following equations for the function $U(\rho)$ [cf. Eq. (16)] and parameter μ:

$$\frac{d^2U}{d\rho^2}+\frac{1}{\rho}\frac{dU}{d\rho}-\frac{U}{\rho^2}-\beta U+\frac{2}{3}U^3-\frac{8}{15}U^5=0, \tag{24}$$

$$\int_0^\infty \frac{\partial\langle L\rangle}{\partial\mu}d\rho=0. \tag{25}$$

It should be noted that the solution U to Eq. (24) depends on the parameter β [defined in Eq. (23)], and it is determined by boundary conditions

$$U(\rho;\beta)\approx a(\beta)\rho \quad \text{at } \rho\to 0;$$

$$U(\rho;\beta)\approx A(\beta)\rho^{-1/2}\exp(-\sqrt{\beta}\rho) \quad \text{at } \rho\to\infty \tag{26}$$

with some constants $a(\beta)$ and $A(\beta)$.

Using the notation

$$\varepsilon_j(\beta)\equiv\int_0^\infty U^{2j}(\rho;\beta)\rho\,d\rho, \quad j=1,2,3, \tag{27}$$

we can rewrite Eq. (25) as

$$\int_0^\infty\left[\left(\frac{dU}{d\rho}\right)^2+\frac{U^2}{\rho^2}\right]\rho\,d\rho=\left(\frac{\mu^2}{3}-k\right)\varepsilon_1+\frac{1}{3}\varepsilon_2-\frac{8}{45}\varepsilon_3. \tag{28}$$

Also, Eq. (24) can be converted into the equivalent form,

$$\left[\left(\frac{dU}{d\rho}\right)^2+\frac{U^2}{\rho^2}\right]\rho=\frac{d}{d\rho}\left(\rho U\frac{dU}{d\rho}\right)-\beta\rho U^2+\frac{2}{3}\rho U^4-\frac{8}{15}\rho U^6. \tag{29}$$

After substitution of Eq. (29) into Eq. (28), one should integrate the right-hand side of Eq. (29) over ρ, the integral of the first term vanishing due to the boundary conditions (26). This procedure results in an implicit functional relationship between μ and β:

$$\mu^2(\beta)=\varepsilon_1^{-1}(\varepsilon_2-16\varepsilon_3/15), \tag{30}$$

which, considering the definition (23), yields $k(\beta)=\beta-(\varepsilon_2-16\varepsilon_3/15)/3\varepsilon_1$.

Using the shooting method, we have found soliton solutions to Eq. (24) for different values of β, which are displayed by the dashed curves in Fig. 4. Note that the comparison between the solid and dashed curves, representing the soliton profiles as produced by the two different *Ansätze* introduced above (based, respectively, on the spherical and cylindrical coordinates), makes sense at $\tau=0$, when the spatiotemporal and spatial radial variables r and ρ coincide. It is also noteworthy that the maxima of the slope at the origin for both approximate solutions are attained at $k\approx 0.09$.

Next, we calculated the values ε_j [Eq. (27)], μ [Eq. (30)], and, lastly, k. This allows us to construct the dependencies $\varepsilon_j(k)$, $\mu^{-1}(k)$, and $\beta^{-1/2}(k)$, which are shown in Fig. 8. Note that the behavior of the soliton temporal width μ^{-1} differs considerably from that of its spatial width $\beta^{-1/2}$ [the widths may be interpreted this way according to the asymptotic expressions (26)]. Such a difference is possible because of a fast increase of the asymptotic amplitude $A(\beta)$ with β. The minimum of the temporal width μ^{-1}, clearly seen in Fig. 8, occurs at $k\simeq 0.067$, when $\mu^2\simeq\beta$.

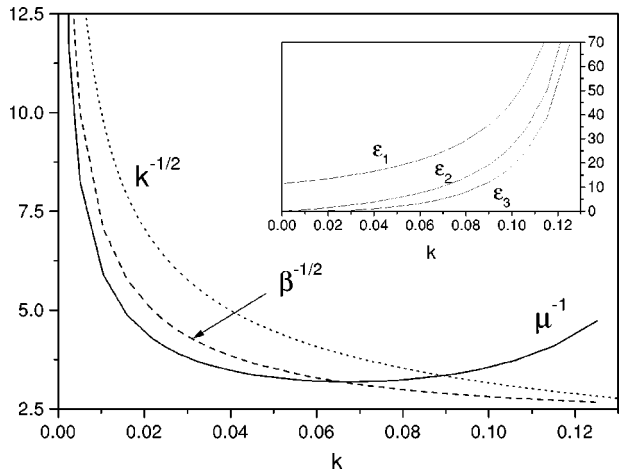

FIG. 8. The values ε_j, μ^{-1}, and $\beta^{-1/2}$ defined as per, respectively, Eqs. (27), (30), and (23), vs k. For comparison, the curve $k^{-1/2}$ is also shown.

It is now possible to evaluate the energy of the soliton, as per the present version of the VA,

$$E(\mu,\beta)=2\pi\int_{-\infty}^{\infty}\mathrm{sech}^2(\mu\tau)d\tau\int_0^\infty U^2(\rho;\beta)\rho\,d\rho$$
$$=4\pi\mu^{-1}\varepsilon_1(\beta). \tag{31}$$

The energy as a function of k is shown in Fig. 5. The minimum of the energy coincides with that at $k=0.033$, predicted by the previous version of the VA (the minimum energy itself is $E_{\min}/4\pi\approx 57$). So the two very different *Ansätze* predict almost identical stability borders for the spinning 3D solitons. However, it is seen from Fig. 5 that the energy predicted by the cylindrical *Ansätze* (21) grows faster than that predicted by the spherical one (15). It was possible to find numerical solutions to Eq. (24) only for $k<0.14$. Thus, the upper existence limit for the spinning solitons as per the cylindrical *Ansätze* is slightly less than the above limit $k_{\max}=0.15$ generated by the spherical *Ansätze*.

The field distributions predicted by the two different trial functions (15) and (21), at two different values of k, can be compared by looking at Figs. 6 ($k=0.045$, $\mu^2>\beta$) and 7 ($k=0.125$, $\mu^2<\beta$). From these results, we conclude that the VA predicts the energy of the multidimensional spinning solitons better than details of their shape (note that the analysis of the VA for 1D and 2D solitons in the model with quadratic nonlinearity led to a similar general conclusion [32]).

IV. CONCLUSION

In this work, we sought for 3D soliton solutions in a model of media with self-focusing cubic and self-defocusing quintic nonlinearities. Numerically exact solutions for the solitons without spin, and variational solutions (using two

different versions of the variational approximation, which yield fairly close final results) for the spinning solitons were obtained. We predict the existence of two branches in the dependence of the 3D soliton's energy vs its propagation constant k for both types of solitons. One of these branches corresponds to stable solitons, and the other to unstable ones. The region of existence of stable solitons is found to be slightly narrower for the spinning solitons: the bottom border is at $k \approx 0.033$ for the spinning solitons, and at $k \approx 0.026$ for the zero-spin ones. The top existence borders almost exactly coincide for both types of soliton. Comparison with the known results for 2D vortex solitons [13] suggests that the top border is lowered with increase of the dimension from 2 to 3. A noteworthy common property of the solitons in this model is that, almost irrespective of the dimension ($D=2$ or $D=3$), the minimum (threshold) energy necessary for the formation of a soliton with spin 1 exceeds by more than four times the minimum energy necessary to create a spinless soliton.

It still remains to test the stability of the spinning soliton in direct four-dimensional numerical simulations.

Note added in proof. Very recently, direct numerical simulations of the spinning light bullet (with the values of the spin 1 and 2) in the present (cubic-quintic) model were performed by D. Mihalache, D Mazilu, L.-C. Crasovan, B. A. Malomed, and F. Lederer (unpublished). The result is that, strictly speaking, the spinning bullet is always unstable against azimuthal perturbations, which eventually leads to splitting of the bullets into a set of several flying nonspinning ones, the initial spin being converted into the net orbital momentum of the ''splinters.'' However, depending on the initial energy of the spinning bullet, it may persist over a fairly long propagation distance (many soliton periods) before the actual onset of the instability. In some cases, the quasistable-propagation distance turns out to be so long that the spinning bullet is virtually stable from the standpoint of any possible experiment. Thus, the spinning bullets considered in the present paper are quite meaningful physical objects.

ACKNOWLEDGMENTS

Useful discussions with N. N. Rozanov and F. W. Wise are appreciated. We are indebted to M. Quiroga-Teixeiro for the preprint of Ref. [27]. This work has been supported in part by INTAS (European Union) under Grant No. 96-0339.

[1] A. A. Kanashov and A. M. Rubenchik, Physica D **4**, 122 (1981).
[2] J. T. Manassah, P. L. Baldeck, and R. R. Alfano, Opt. Lett. **13**, 1090 (1988).
[3] Y. Silberberg, Opt. Lett. **15**, 1282 (1990).
[4] A. B. Blagoeva, S. G. Dinev, A. A. Dreischuh, and A. Naidenov, IEEE J. Quantum Electron. **QE-27**, 2060 (1991).
[5] K. Hayata and M. Koshiba, Phys. Rev. Lett. **71**, 3275 (1993).
[6] K. Hayata and M. Koshiba, Phys. Rev. E **48**, 2312 (1993).
[7] X. Liu, L. J. Qian, and F. W. Wise, Phys. Rev. Lett. **82**, 4631 (1999).
[8] D. E. Edmundson and R. H. Enns, Phys. Rev. A **51**, 2491 (1995).
[9] D. E. Edmundson and R. H. Enns, Opt. Lett. **18**, 1609 (1993).
[10] R. H. Enns, D. E. Edmundson, S. S. Rangnekar, and A. E. Kaplan, Opt. Quantum Electron. **24**, S1295 (1992).
[11] R. McLeod, K. Wagner, and S. Blair, Phys. Rev. A **52**, 3254 (1995).
[12] B. A. Malomed, P. Drummond, H. He, A. Berntson, D. Anderson, and M. Lisak, Phys. Rev. E **56**, 4725 (1997); D. Mihalache, D. Mazilu, B. A. Malomed, and L. Torner, Opt. Commun. **152**, 365 (1998); D. Michalache, D. Mazilu, J. Dörring, and L. Torner, *ibid.* **159**, 129 (1999).
[13] M. Quiroga-Teixeiro and H. Michinel, J. Opt. Soc. Am. B **14**, 2004 (1997).
[14] B. A. Malomed, Phys. Rev. E **58**, 7928 (1998).
[15] A. S. Desyatnikov and A. I. Maimistov, Zh. Eksp. Teor. Fiz. **113**, 2011 (1998) [JETP **86**, 1101 (1998)]; A. Maimistov, B. Malomed, and A. Desyatnikov, Phys. Lett. A **254**, 179 (1999).
[16] M. R. Belić, A. Stepken, and F. Kaiser, Phys. Rev. Lett. **82**, 544 (1999).
[17] F. Wise (private communication).
[18] V. S. Butylkin, A. E. Kaplan, Yu. G. Khronopulo, and E. L. Yakubovich, *Resonant Nonlinear Interactions of Light with Matter* (Springer-Verlag, Berlin, 1989).
[19] A. W. Snyder, D. J. Mitchell, L. Poladian, and F. Landouceur, Opt. Lett. **16**, 21 (1991).
[20] V. Tikhonenko, J. Christou, and B. Luther-Davies, Phys. Rev. Lett. **76**, 2698 (1996).
[21] M. G. Vakhitov and A. A. Kolokolov, Izv. Vyssh. Uchebn. Zaved., Radiofiz. **16**, 1020 (1973) [Sov. J. Radiophys. Quantum Electron. **16**, 783 (1973)].
[22] D. E. Edmundson, Phys. Rev. E **55**, 7636 (1997).
[23] J. Atai, Y. Chen, and J. M. Soto-Crespo, Phys. Rev. A **49**, R3170 (1994).
[24] K. Hayata and M. Koshiba, Phys. Rev. E **51**, 1499 (1995).
[25] B. L. Lawrence, M. Cha, J. U. Kang, W. Torruellas, G. Stegeman, G. Baker, J. Meth, and S. Etemad, Electron. Lett. **30**, 889 (1994).
[26] A. A. Kolokolov, Izv. Vyssh. Uchebn. Zaved., Radiofiz. **17**, 1332 (1974) (in Russian).
[27] A. Berntson, M. Quiroga-Teixeiro, and H. Michinel, J. Opt. Soc. Am. B **16**, 1697 (1999).
[28] V. I. Kruglov, Yu. A. Logvin, and V. M. Volkov, J. Mod. Opt. **39**, 2277 (1992).
[29] W. J. Firth and D. V. Skryabin, Phys. Rev. Lett. **79**, 2450 (1997).
[30] D. V. Petrov and L. Torner, Opt. Quantum Electron. **29**, 1037 (1997).
[31] D. V. Petrov, L. Torner, J. Martorell, R. Valaseca, J. P. Torres, and C. Cojocaru, Opt. Lett. **23**, 1444 (1998).
[32] V. Steblina, Yu. S. Kivshar, M. Lisak, and B. A. Malomed, Opt. Commun. **118**, 345 (1995).
[33] E. A. Kuznetsov, A. M. Rubenchik, and V. E. Zakharov, Phys. Rep. **142**, 105 (1986).
[34] J. C. Neu, Physica D **43**, 385 (1990).
[35] C. De Angelis, IEEE J. Quantum Electron. **QE-30**, 818 (1994); K. Dimitrevski, E. Reimhult, E. Svenson, A. Öhgren, D. Anderson, A. Berntson, M. Lisak, and M. Quiroga-Teixeiro, Phys. Lett. A **248**, 369 (1998).